

UNCLASSIFIED

AD NUMBER
ADB229334
NEW LIMITATION CHANGE
TO Approved for public release, distribution unlimited
FROM Distribution authorized to U.S. Gov't. agencies only; Specific Authority; Sep 97 Other requests shall be referred to Commander, Army Medical Research and Development Command, Attn: MCMR-RMI-S Fort Detrick, Frederick, MD 21702-5012.
AUTHORITY
USAMRMC ltr, 4 Dec 2002

THIS PAGE IS UNCLASSIFIED

AD _____

CONTRACT NUMBER DAMD17-97-C-7008

TITLE: Sensitive, Specific Complementary - Strand Optical
Detection of Viral RNA

PRINCIPAL INVESTIGATOR: Ronald J. Rieder, Ph.D.

CONTRACTING ORGANIZATION: VISIDYNE, Incorporated
Burlington, Massachusetts 01803

REPORT DATE: June 1997

TYPE OF REPORT: Final - Phase I

PREPARED FOR: Commander
U.S. Army Medical Research and Materiel Command
Fort Detrick, Frederick, Maryland 21702-5012

DISTRIBUTION STATEMENT: Distribution authorized to U.S.
Government agencies only (specific authority). Other requests
for this document shall be referred to Commander,
U.S. Army Medical Research and Materiel Command, ATTN:
MCMR-RMI-S, Fort Detrick, Frederick, MD 21702-5012

The views, opinions and/or findings contained in this report are
those of the author(s) and should not be construed as an official
Department of the Army position, policy or decision unless so
designated by other documentation.

19970919 084

DTIC QUALITY INSPECTED 4

REPORT DOCUMENTATION PAGE

Form Approved
OMB No. 0704-0188

Public reporting burden for this collection of information is estimated to average 1 hour per response, including the time for reviewing instructions, searching existing data sources, gathering and maintaining the data needed, and completing and reviewing the collection of information. Send comments regarding this burden estimate or any other aspect of this collection of information, including suggestions for reducing this burden, to Washington Headquarters Services, Directorate for Information Operations and Reports, 1215 Jefferson Davis Highway, Suite 1204, Arlington, VA 22202-4302, and to the Office of Management and Budget, Paperwork Reduction Project (0704-0188), Washington, DC 20503.

1. AGENCY USE ONLY (Leave blank)		2. REPORT DATE June 1997	3. REPORT TYPE AND DATES COVERED Final-Phase I (11 Nov 96 - 10 May 97)	
4. TITLE AND SUBTITLE Sensitive, Specific Complementary - Strand Optical Detection of Viral RNA			5. FUNDING NUMBERS DAMD17-97-C-7008	
6. AUTHOR(S) Ronald J. Rieder, Ph.D.				
7. PERFORMING ORGANIZATION NAME(S) AND ADDRESS(ES) VISIDYNE, Incorporated Burlington, Massachusetts 01803			8. PERFORMING ORGANIZATION REPORT NUMBER	
9. SPONSORING/MONITORING AGENCY NAME(S) AND ADDRESS(ES) Commander U.S. Army Medical Research and Materiel Command Fort Detrick, Frederick, Maryland 21702-5012			10. SPONSORING/MONITORING AGENCY REPORT NUMBER	
11. SUPPLEMENTARY NOTES				
12a. DISTRIBUTION / AVAILABILITY STATEMENT Distribution authorized to U.S. Government agencies only (specific authority). Other requests for this document shall be referred to Commander, U.S. Army Medical Research and Materiel Command, ATTN: MCMR-RMI-S, Fort Detrick, Frederick, Maryland 21702-5012.			12b. DISTRIBUTION CODE	
13. ABSTRACT (Maximum 200) The feasibility of a novel low-cost sequence-specific nucleic acid detector of great speed and dynamic range has been examined and each system component has been tested to confidence. This detector records binding events at the surface of optical waveguides, through coupling to the evanescent wave. The detector is made possible through innovative phase measurement techniques practiced by Visidyne. The laboratory design exceeds current detection noise thresholds and holds great promise. Its components have been characterized and proven to show unparalleled sensitivity; in addition, an innovative method for improving sensitivity a thousand times is presented. The novel detection and bandpass filtering techniques exceed the state of art in evanescent-wave biosensing technology. Development of this system requires technical mastery in many disciplines; therefore, diverse concepts and data are discussed. The results suggest a likely strategy by which the system components, biochemical and electronic can be integrated to form a revolutionary new technique for chemical sensing.				
14. SUBJECT TERMS RNA, enterovirii, biosensor, evanescent waves, refractometry, phase detection, complementary strand hybridization			15. NUMBER OF PAGES 31	
			16. PRICE CODE	
17. SECURITY CLASSIFICATION OF REPORT Unclassified	18. SECURITY CLASSIFICATION OF THIS PAGE Unclassified	19. SECURITY CLASSIFICATION OF ABSTRACT Unclassified	20. LIMITATION OF ABSTRACT Limited	

FOREWORD

Opinions, interpretations, conclusions and recommendations are those of the author and are not necessarily endorsed by the U.S. Army.

____ Where copyrighted material is quoted, permission has been obtained to use such material.

____ Where material from documents designated for limited distribution is quoted, permission has been obtained to use the material.

RJR Citations of commercial organizations and trade names in this report do not constitute an official Department of Army endorsement or approval of the products or services of these organizations.

____ In conducting research using animals, the investigator(s) adhered to the "Guide for the Care and Use of Laboratory Animals," prepared by the Committee on Care and Use of Laboratory Animals of the Institute of Laboratory Resources, National Research Council (NIH Publication No. 86-23, Revised 1985).

____ For the protection of human subjects, the investigator(s) adhered to policies of applicable Federal Law 45 CFR 46.

____ In conducting research utilizing recombinant DNA technology, the investigator(s) adhered to current guidelines promulgated by the National Institutes of Health.

____ In the conduct of research utilizing recombinant DNA, the investigator(s) adhered to the NIH Guidelines for Research Involving Recombinant DNA Molecules.

____ In the conduct of research involving hazardous organisms, the investigator(s) adhered to the CDC-NIH Guide for Biosafety in Microbiological and Biomedical Laboratories.

 6-10-97

PI - Signature Date

Table of Contents

Overview of Phase I Results	2
Theory and Construction	3
Optical Basis for the Signal	3
Biochemical design	4
Mechanical Interferometer Development	8
Electronics Construction	10
Laser Diode (10)	
Precision Phase Measurements (10)	
Tri-Phase Detection Method. (11)	
Phase Detectors (12)	
Phase Processor Board (13)	
Laboratory Experiments	15
Noise Characterization	15
Protein Binding	16
Discussion	17
Noise sources	17
Sources of Signal Loss	17
Existing Applications of Biosensors; Sensitivity Projections	20
Differential measurement	24
Temporal Discrimination (24)	
Bandpass Filtering (25)	
Polarization Modulators (27)	
Conclusions	27
References	27
Personnel	28

Overview of Phase I Results:

Visidyne, Inc. has proposed the development of a novel biosensor with sensitivity and specificity in excess of any comparable instrument. The phase I proposal asserted that Visidyne, as a consequence of its already known and proven ability to make measurements of optical phase with unequaled sensitivity and speed, had in its hands the necessary technology for breaking new ground in chemical and biochemical sensing. Visidyne entered the Phase I effort for this solicitation confident that, we could develop technology enabling unprecedented physical resolution in the measurement of optical phase changes due to analyte binding, as used by *existing* evanescent wave biosensors. With the preliminary work of the Phase I, we have rapidly and thoroughly demonstrated that indeed we can bring the promised resolution to bear on this problem; we have achieved a degree of physical sensitivity unheard of in the field and corresponding to *picometers* of difference in optical phase; in addition we have established the feasibility of implementing differential techniques to resolve *Ångstroms*. The unprecedented sensitivity -- comparable "biosensing" efforts measure optical distances on the order of tens of nanometers -- has been achieved on a realistic sensing platform, in real laboratory conditions as faced by medicinal chemists, field workers and molecular biologists, rather than with the luxury of the optical bench. This success is coupled with the ability to ignore thermal and vibrational noise sources which plague other groups working in this realm, and, taken with our successful chemistry and molecular biology, positions us to obtain measurements leaps and bounds ahead of those any other research facility can make -- in environments which are realistic both in terms of their poor chemical characterization and their uncontrolled thermal and vibrational noise. As a consequence of the Phase I work the elements needed in developing this sensor have been separated, optimized, and *proven*, and it remains only to assemble these components into a single deliverable unit.

The complexity of the project, requiring as it does expertise across many disciplines, rigid use constraints, and advanced electronics, has proved a formidable challenge through the effort. The research team has encountered problems as mundane as difficulties in implementing the novel miniature laser source used for this work, and as esoteric as subtleties in the polarization state of the incident light. In some cases the unprecedented sensitivity of our measurement has led us to discover problems others have not yet had to overcome, *e.g.* phase drifts in the lasing source; in surmounting these difficulties we have opened up new possibilities for this kind of chemical detection. In other cases our own knowledge of the field was insufficient, and we chose to operate in domains where the signal would be less strong -- in particular working at lower indices of refraction in our waveguides, and working in "ray" rather than "modal" regions where our signal was small even for our sensitivity. The contacts we have established in the field, and our own developed expertise in biosensing, have made clear physical methods to improve signal strength *without* compromising our astonishing noise insensitivity.

As a consequence of these and other difficulties the ambitious schedule of the phase I proposal was not fully realized; realistic measurements characterizing the construction of the interferometer were made but they do not extend to solving fully the problem posed by the solicitation, yet. However as a consequence of the phase I work Visidyne has acquired a mastery of problem and can outline a clear path to resolve the remaining obstacles and indeed to improve on the proposed phase I design in a number of ways, including a bandpass filtering technique so unique and promising that it is detailed further below under *Discussion*. Below we will present the nature of these difficulties and the course Visidyne has charted to address them in what is now, because of the measurements made during the

phase I, a straightforward problem of assembling existing and proven technologies.

Theory and Construction:

Optical Basis for the Signal. Our measurement technique looks for effects which occur within the *evanescent wave* surrounding the optical waveguides; this phenomenon is described below and has been understood well for two centuries.

When light impinges on the boundary between two transparent media of different indices of refraction -- say water and air -- in general it gives rise to a reflected wave and a transmitted wave, as shown in figure 1. In this figure we imagine light passing from a more optically dense medium, into a less dense medium. Note that the transmitted ray is refracted: bent toward the surface so that the angle between the transmitted ray and the surface is shallower than that of the incident and reflected rays. As the incident ray is brought closer to the surface the angle becomes still shallower until the transmitted ray is essentially propagated *along the interface*, no longer sending energy into the new medium, so that all the energy of the incident ray is losslessly incorporated into the reflected ray; this phenomenon is called total internal reflection. When we consider events on a small scale it is no longer helpful to describe this phenomenon with rays, but rather as propagating waves or modes; in this picture the transmitted ray, when it propagates along the surface, becomes a evanescent standing wave, like a plucked string, vibrating along the interface. The magnitude of this wave dies off exponentially with the distance from the surface and scales linearly with the light wavelength. Its wavelength and phase are all dependent on the environment at the interface, at least within that region where its magnitude is big. Since the incident, reflected and evanescent waves all oscillate in step, changes in the local phase of the evanescent wave result in changes in the phase of the reflected wave; thus the reflected wave phase depends in part on the environment at the interface.

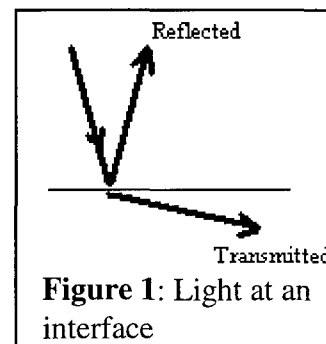


Figure 1: Light at an interface

Our design couples light into a glass prism and subjects it to total internal reflection three times -- as the device is miniaturized this will become hundreds of times -- with the emerging, multiply-reflected beam sent to Visidyne's phase processing electronics, which are capable of resolving extremely small changes in the phase as described below.

There exist some subtleties in this process. The phase shift in the transmitted wave is a function of the index of refraction (or dielectric constant) experienced by the evanescent wave, which, in our design, is affected by binding events happening at the surface of the prism.

The reflected wave phase shift, however, is also a function of the incident wave polarization, relative to the plane of the interface. If the incident state of polarization is not exactly parallel or perpendicular to the reflective surface, its parallel and perpendicular components are phase shifted differently -- in practice that means linearly polarized light can become circularly polarized and circularly polarized light can become linearly polarized. Fig 2 below shows a plot of the *difference* in phase shift for the

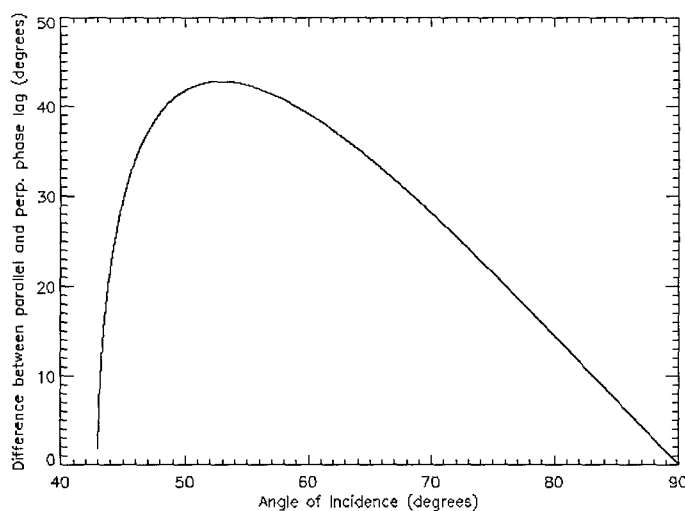


Figure 2: Difference of effect upon orthogonal polarization components

parallel component, and for the perpendicular component, of incident light as a function of incidence angle at the waveguide surface, presuming a waveguide index of 1.95 and a water index of 1.33; this difference naturally goes to zero at the critical angle for total internal reflection (here about 43°) and at 90° . This effect, too, is dependent on binding events in the external medium. Because light with different polarization states does not interfere, there are two implications for the Visidyne biosensor as regards polarization. Firstly, that the polarization state of the light must be understood and controlled, or the resulting signal will have poor modulation depth and therefore our signal-to-noise will be much reduced. Secondly, that, in the ultimate design of our instrument, we can use this effect to generate a differential signal and hence to improve our signal-to-noise. This possibility, of increasing signal-to-noise through creating a differential signal and bandwidth filtering, will be discussed further below.

Another subtlety relates to the waveguide index of refraction. The waveguide itself must have substantially greater index of refraction, than the protein/silane coating: the phase shift depends strongly on this difference. Therefore choice of the appropriate glass waveguide is crucial for a good signal. However there is some guesswork involved in this process since we have little *a priori* information about the optical properties of the silane; as the biosensor evolves the waveguide material must become more carefully tailored to the problem.

Biochemical design: A trial system for attaching probe nucleic acids to the optics needed to be designed for the phase I trials. Ideally, one would like to synthesize nucleic acids directly onto the optical surface to minimize the possibility of nonspecific interactions, to enhance sensitivity, and to covalently fix the probe onto the surface to avoid cross-contamination and leaching. Chemistries for this synthesis exist; nucleic acids have been synthesized directly onto fiber optics for fluorescence based detectors and for "DNA chip" arrays used in genome screening; the latter techniques are particularly attractive because their incorporation of microchip-like photolithographic techniques enables precise physical localization of the probe and is conducive to miniaturization of the device.

We were interested in running tests with both PNA and DNA probes. PNAs are a new and exciting

synthetic compound that has the potential for conferring a better sensitivity and immunity to chemical environment. These are polymers with nucleic acid side chains but uncharged peptide, rather than sugar-phosphate, backbones, and alternating glycines. PNAs can bind complementary sequence with 1000-fold lower K_d than DNA, hybridize well to both A and B form nucleic acids due to the conformational flexibility of its backbone [Egholm, 1993] and some previous work on PNA based detection [Wang, 1996] indicates that it is not only very sensitive but remains so across a wide range of buffer ionic strengths and pH, making PNA ideal for a field instrument. The great affinity of PNAs for complementary sequence generally results in the use of shorter probes and therefore greater sensitivity to mismatches.

There exist some difficulties in directly synthesizing nucleic acids onto the optics. Visidyne, Inc. is not well equipped to synthesize nucleic acids and cannot become so equipped under the time and expense guidelines of the Phase I proposal. Therefore we wished to purchase synthetic oligomers rather than synthesize them *de novo*. In addition, we wished to test two types of nucleic acid as probes: DNA and PNA, discussed. However the PNA peptide backbone and the DNA sugar-phosphate backbone are quite different chemically and therefore at least two synthetic protocols would be required. Lastly we wished to have some flexibility in the probe sequences used; once a sequence is covalently attached to the slide surface it cannot be easily changed. Therefore we wished a sort of "universal coupling" to attach nucleic acids to the slides.

The solution we chose, was to purchase biotinylated nucleic acids -- since suppliers of both PNA and DNA will readily biotinylate their oligomers -- and couple these to the optical surface via a covalently coupled protein mediator. We later discovered that the same approach has been used in an evanescent wave sensor before, with avidin as mediator. We chose instead, however, to use goat anti-biotin IgG as a mediator; the anti-biotin offers the following performance advantages over the avidin:

- Smaller size, hence less interference and less reduction of signal
- Possibility of using another immunoglobulin as a corrective for nonspecific binding
- Even tighter binding than avidin
- Proven ruggedness of goat IgG's tethered to glass under long-term storage
- Immediate readiness* to develop immunosensors targeted at other ligands, a primary area of use for the commercialized sensor

The intermediate protein does presumably cause some loss of sensitivity, because it positions the nucleic acid farther away from the optic and hence in a less sensitive region of the evanescent field. However, other groups have made evanescent field measurements in this manner; the Georgia Tech group of Nile Hartman, using avidin, found that concentrations of DNA as low as 0.5 ng/mL -- somewhat poor; however Dr. Hartman's group is measuring phase at 0.01 cycle resolution, whereas Visidyne can measure phase at 0.00001 cycle to 0.0000001 cycle resolution and therefore has optical limits of 0.5 pg/L or even 5 pg/kL -- PCR-like sensitivity!

Using goat IgG as a binding molecule enabled us to do some optimization of the chemistry. Our basic chemical protocol was to (1) wash the glass with concentrated KOH/MeOH, then briefly wash in HCl (the purpose being to leave exposed glass functional groups protonated; sometimes this affects the chemistry), (2) expose the washed glass to a bifunctional silane reagent containing an activated bifunctional methoxysilane (activated to a silanol by mild acetic acid) which would covalently bind to the glass and present an electrophilic group to solution, and (3) incubate the silanized glass with

the immunoglobulin, cross-linking the electrophile onto nucleophilic sites on the protein, ideally the N-terminal (The resulting structure could be further reduced to a Schiff base for additional stability if necessary -- we chose not to do this procedure as it did not appear to affect binding efficiency). Rapid, clean handling was essential to prevent the formation of undesired byproducts.

Figure 3 shows a few silanes we tried for the experiment; these and many others are available from United Chemical Technologies (Bristol, PA), a specialist in silane coupling chemistry. We settled

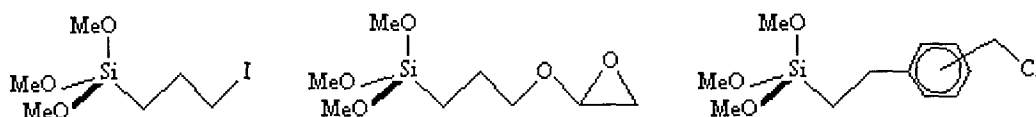


Figure 3: Different bifunctional silanes tried for the experiment

ultimately on the *m,p*-chloromethylphenyl derivative as it showed slightly better activity (assay described below), perhaps due to somewhat greater selectivity for the Fc N-termini; the epoxide was about 0.75-fold as good.

Figure 4 shows a schematic of the surface of the optic, prepared to detect the target RNA. Note that the lasing wavelength is close to a micron so the chemistry is all embedded deep in the surrounding

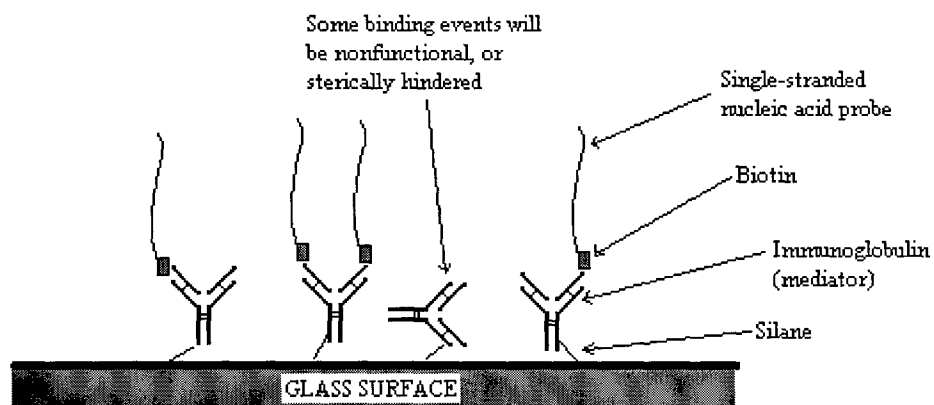


Figure 4: Desired chemistry for feasibility testing of RNA recognition

evanescent standing wave, even though the antibody imposes a minute separation between the glass and the probe. When a target nucleic acid hybridizes onto the probe, that field is perturbed detectably -- if the target is a large molecule like a viral genome or a ribosome, encased in a still larger solvation shell, then the perturbation becomes even more noticeable; however even short oligomers have been detected by this approach.

We optimized our functionalization chemistry by means of a simple biochemical assay. We obtained polyclonal affinity-purified goat anti-Horseradish Peroxidase IgG from Jackson ImmunoResearch Laboratories, Inc (West Grove, PA) and horseradish peroxidase from Sigma. The antibody-coated optics were incubated with horseradish peroxidase in PBS (also the affinity-purification medium), and washed many times in buffer. The amount of bound peroxidase activity on the optic could then be

assayed via any number of commercial colorimetric assays for peroxidase activity; we used a 3, 3', 5, 5' - Tetramethylbenzidine assay with reagents supplied by Biømeda corp. (Forster City, CA). We tried to optimize the total bound activity (relative to a "blank" optic on which we had bound bovine serum albumin rather than immunoglobulin; inevitably this had no activity). This assay was also used on occasion to confirm the continued functionality of optics which had been stored at 4°C for weeks since synthesis.

This assay was particularly appealing in that the measurement reflected the amount of antibody bound but still functional; it is possible for example that the epoxide reagent binds more antibody (and Lowry assays of protein content tentatively confirm this hypothesis), but binds less *functional* antibody -- so here we are making a relevant test. The variables we examined were silane concentration, total mass of silane per sq. cm. of glass, pH of silanization buffer, total amount of antibody per sq. cm. of glass, antibody concentration, buffer composition for antibody binding, and duration of antibody incubation.

All of these factors were to some extent important. As expected, the bound activity increased as the amount of antibody the slide was exposed to increased; surprisingly the activity peaked at about 3µg antibody/sq. cm of glass, and fell off gradually thereafter (Fig. 5). Surface uniformity was assayed by the use of FITC-labeled peroxidase and florescence microscopy; the glass surface was found by this test to be uniformly labeled, with no areas of the glass particularly dense or sparse in protein.

Further optimization of the binding chemistry can and must be done -- in particular to characterize surface uniformity better, to characterize receptor density, and to measure approximate sensing layer depth; these studies will require much more extensive work in the chemistry lab and were considered unnecessary for the phase I effort; however they will constitute an integral part of the phase II.

Target probe selection is naturally important. the considerations appear to be the same, however, as for PCR primers: high T_m , no secondary structure in primer or target, uniqueness of sequence. There are some additional constraints on PNA probes having to do with allowable sequences, length, and more careful avoidance of secondary structure (PNA/PNA duplexes are considerably stronger than PNA/RNA or PNA/DNA duplexes). This process is straightforward for the molecular biologists and we have identified a number of potentially good probe sequences for hepatitis A, various poliovirus strains, and other enterovirii. Thus to DNA primers we chose a few primers from the literature with specificity for various parts of the genome, ran the Whitehead Institute's PRIMER algorithm to determine the characteristics of each, and used NCBI's BLAST sequence alignment tool to verify the uniqueness of each probe site. In addition relevant portions of the viral genomes were examined with the MULFOLD algorithm of the GCG package to verify the likely absence of competing secondary

**Peroxidase activity vs. total amount of goat IgG;
Average of two experiments**

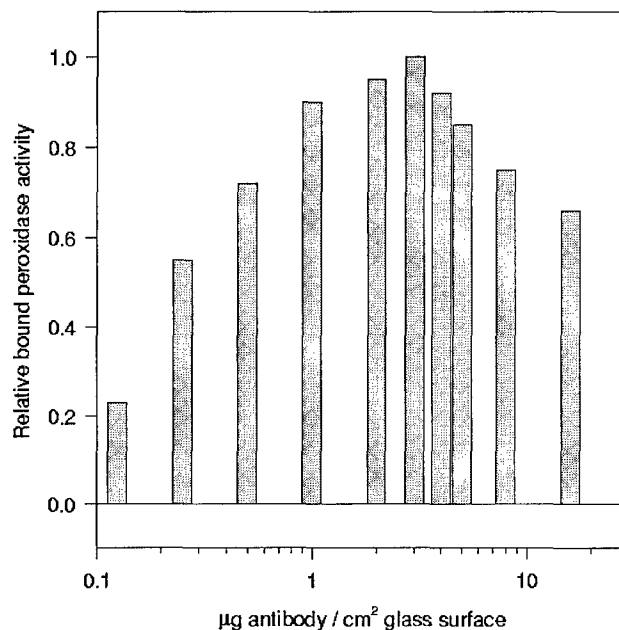


Figure 5: Typical experimental data

structure in the sites chosen; this step is not normally taken in primer selection however since we did not have the luxury of trying many primers it was important to have confidence in the ones we selected. From these primers we then identified substretches of sequence which might make likely PNA probes; PNA probes are necessarily shorter (~15 nt max) so these new sequences had to once again be checked for uniqueness. They also had to meet some special constraints, in particular low purine content; purine rich PNAs tend to aggregate. Viral secondary structure is less troubling (PNAs can easily invade duplexes or can where appropriate form triplex structures through reverse Hoogsteen pairing) but naturally since the PNA probes were taken from within the DNA probe sequences it is anticipated that their target sequences are wholly or partially exposed. We chose primers for use with poliovirus as a first step towards the detection of enteroviral RNA; this system has been used in the literature [Egger, 1995; Abraham, 1993] as a test system for enteroviral detection and has a few advantages for Visidyne: a few serotypes are commercially available, the genomes are well-characterized, and there is little hazard in handling the material.

Mechanical Interferometer Development. As part of the Phase I effort Visidyne has developed and characterized a quasi-cyclic self-compensating interferometer. Because Visidyne presently does not have the facilities needed to do chemistry or biology in-house a “workstation” configuration was chosen to demonstrate feasibility in anticipation of having to conduct experiments outside of Visidyne. (Based on the success and potential of this project Visidyne is planning to equip a small laboratory area for chemistry work.) This configuration was also chosen because of the accessibility of the different optical components and its self contained nature which provides a simple platform to understand better the system.

A schematic of the platform is shown in Figure 6; the entire platform is on 12" x 16" in size. The sensor consists of a small laser diode operating in the visible region (690 nm) incident on a beamsplitter that divides the beam into two beams. One of the beams passes directly through beamsplitter and onto the bottom sensing optic immersed in solute. (Two sensing optics are mounted in a removable stainless steel vessel used to contain the solute.) This beam is totally internally reflected within the sensing optic and exits directed onto a roof prism that both folds the beam 90° and elevates it to a higher geometric plane where it remains. It is then folded one more time and directed to a tri-phase detector.

The other beam follows an almost reciprocal path (hence the name “quasi-cyclic”) starting out in the lower geometric plane and elevated to the upper plane by the roof prism *before passing through the sensing optic so as to be incident on the top sensing optic*. Thus the beam passes through an independent sensing optic chemically similar but lacking target specificity, thus subject to the same *nonspecific* interactions. It then exits and is folded by the beamsplitter onto the tri-phase

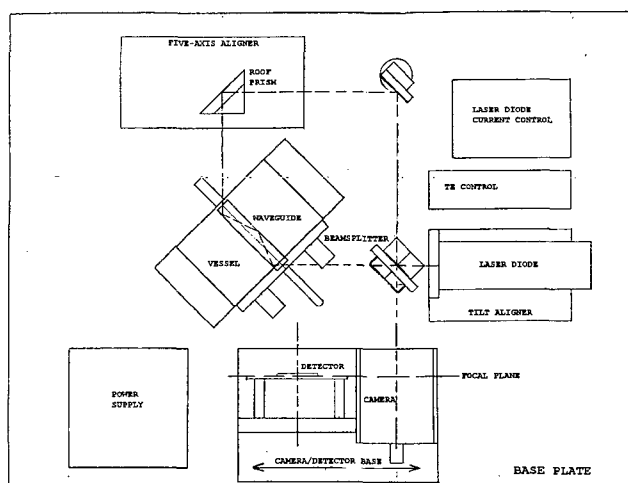


Figure 6.:Schematic drawing of a quasi-cyclic interferometer

detector where the two beams interfere and their relative phase difference is determined. *Measuring the phase between the two independent beams provides, through optical subtraction, the specificity so crucial to the success of any biosensor.*

Laboratory Interferometer. Figures 7 and 8 are photographs of the assembled biosensor workstation and its associated vessel, respectively.

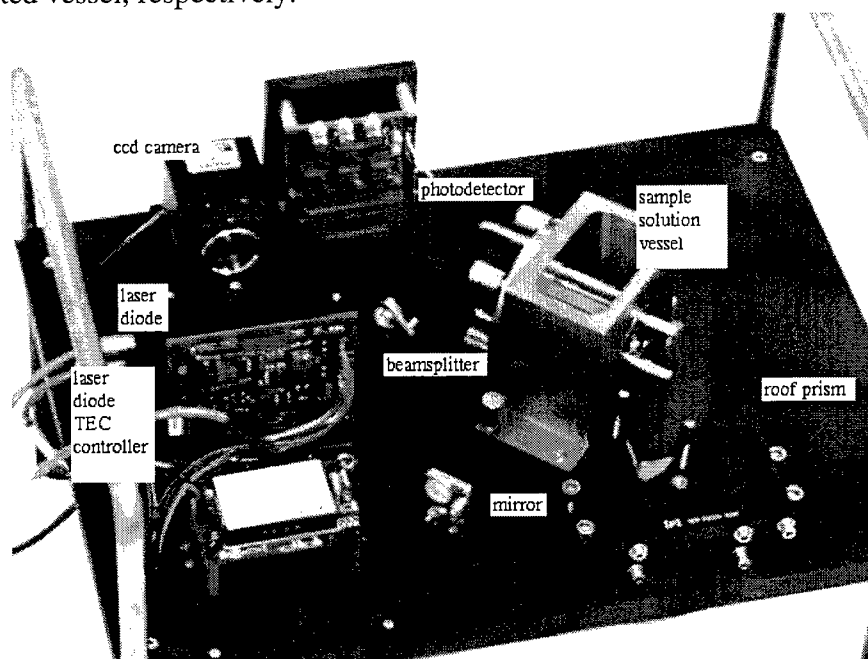


Figure 7: "Workstation" configuration for feasibility experiment

The vessel which contains the target solution and holds the sensitive optics has been designed for maximum optical stability and minimum effort when changing out sensing waveguides. The waveguides are held in a protective basket and are secured in the side of the vessel with four finger tightened screws; the waveguides per se are clamped with two finger screws. All surfaces are pinned for unambiguous orientation, gasketed, and autoclavable. Figure 8 shows (from left to right) the protective basket holding the waveguides, the vessel, and lid.

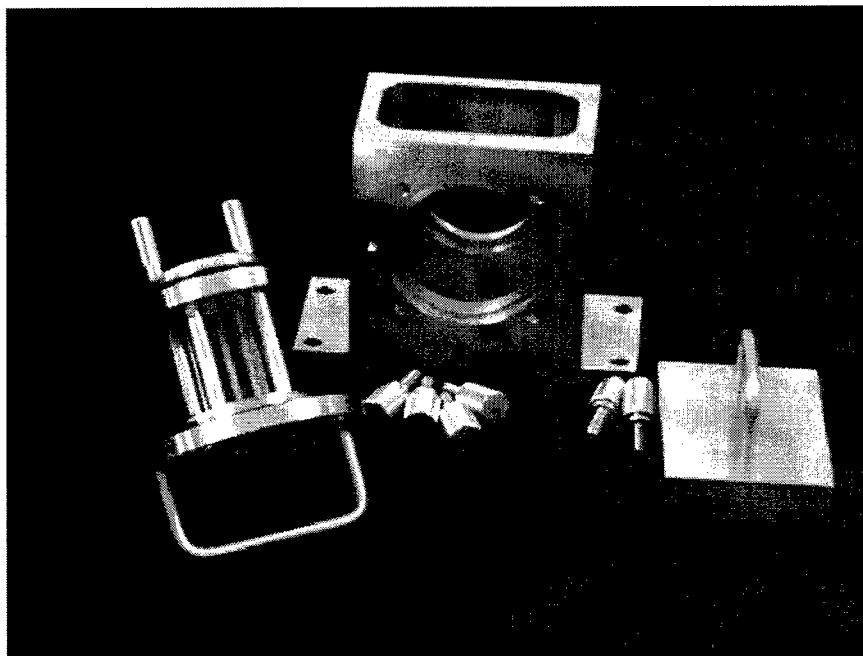


Figure 8: Mount for waveguide optics and reaction vessel

Electronics Construction: The electronic signal processing represents Visidyne's major contribution to the field of biosensing and its core technology; therefore the theory and construction will be discussed in some great detail below.

Laser Diode. A 20 mW 690nm thermoelectrically cooled diode laser was purchased from Micro Laser Systems of Garden Grove, CA and was used as a coherent light source. The wavelength was chosen for its compatibility with silicon detectors, its low cost, availability, and ease in alignment. The laser diode was packaged with appropriate foreoptics to produce a small circular collimated beam less than 2 mm in diameter to be compatible with the size of the sensing optics. In order to stabilize the wavelength of the laser diode a small current controlled power supply as well as a thermoelectric controller were also purchased from the laser supplier and can be seen in the lower lefthand corner of Figure 7.

Precision Phase Measurements. The significant improvement over other phase based optical systems is Visidyne's ability to make precision phase measurements ($<10^{-6}$ cycles). This has the capability of increasing the sensitivity of existing phase based biosensor measurements ($\sim 10^{-3}$ cycles) by several orders of magnitude to sensitivities commensurate with PCR techniques. The high sensitivity measurements of the index of refraction made during this Phase I effort are based on detecting the relative optical phase between light traveling along two different paths with great precision. Such a capability has been developed at Visidyne and a schematic diagram of the technique is shown in Figure

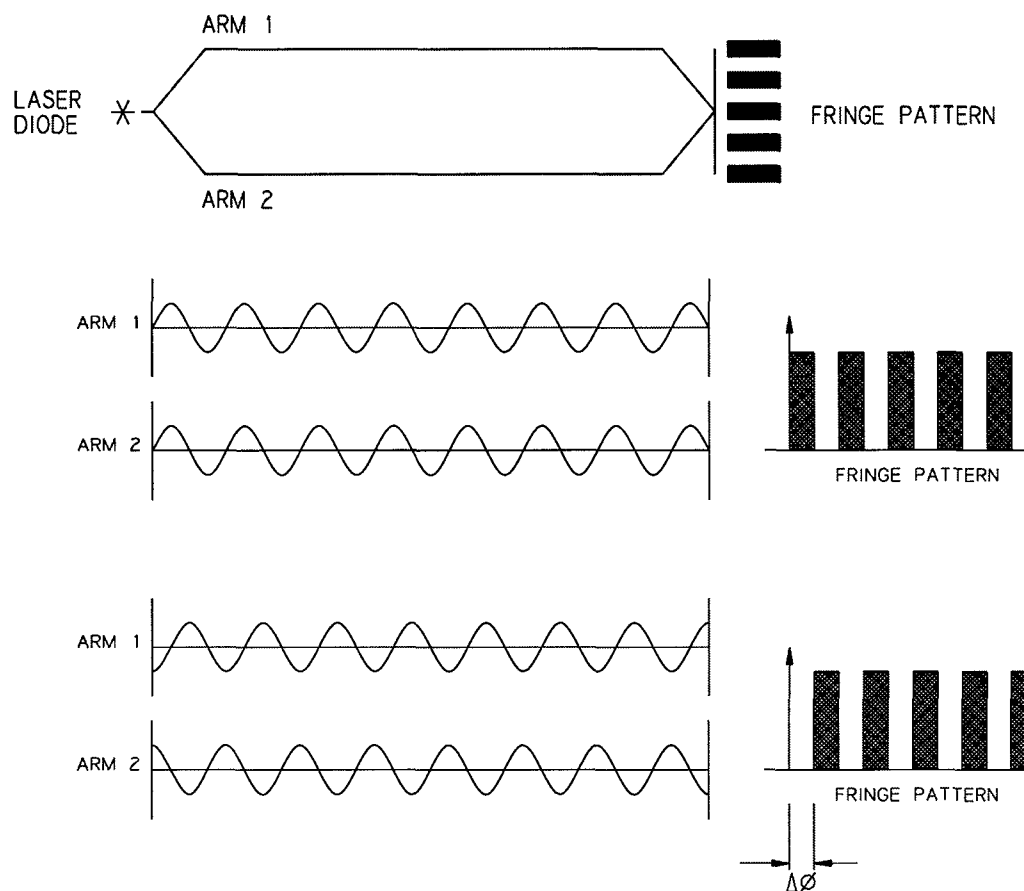


Figure 9: Schematic for Phase Detection

9.

Figure 9a shows a coherent light source divided into two different beams representing two arms of an arbitrary interferometer. A distinction is made that the two arms are then recombined at a small angle hence forming a spatial interference pattern. If both arms of the device are equal in optical path length, both will contain an identical number of wavelengths and the relative phase between the arms will be zero. The result is the stationary interference pattern shown in Figure 9b. However, if the path length of one arm is increased by a known amount, the two arms will contain different numbers of wavelengths and will have different phases when recombined. This results in an interference pattern similar to the equal path case but translated in position. This shift is a direct measure of the relative phase between the two arms and is shown in Figure 9c.

The relationship between the relative phase $\delta\phi$ of the two arms is given by the simple formula

$$\delta\phi = \frac{OPD}{\lambda}$$

where OPD is the optical path difference and λ is the laser wavelength. If the OPD is well known then the lasing wavelength can also be determined with great accuracy. Conversely, if λ is well known then the OPD can be accurately determined.

Tri-Phase Detection Method. The power inherent in the Visidyne method is derived from the ability to determine $\delta\phi$ at the photon noise limit of the laser beam. This results because $\delta\phi$ is determined from simultaneous measurements which are ratioed hence canceling any common noise sources. Consequently, the uncertainty in $\delta\phi$ depends only on the fluctuations from the photon counting statistics and not the laser amplitude noise (the usual limiting factor).

The sinusoidal intensity pattern of an interference fringe is measured at three different positions as shown in Figure 10.

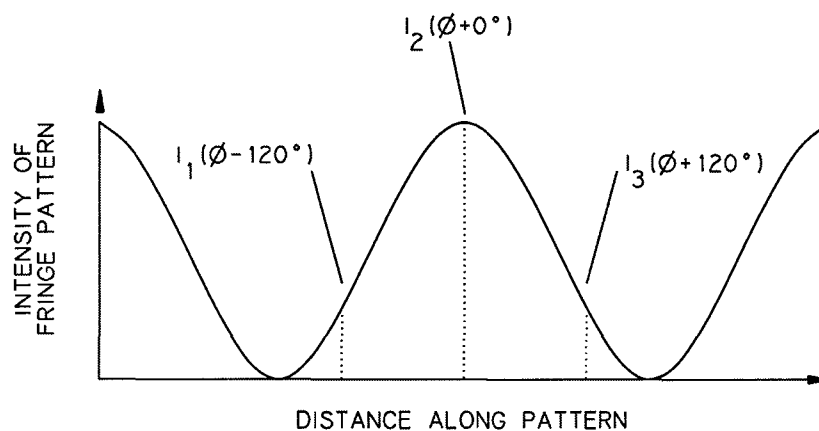


Figure 10: Detection Scheme for Phase Determination

The result are three equations I_1 , I_2 , I_3 and three unknowns I_o , I_r from which ϕ can be obtained.

$$\begin{aligned} I_1 &= I_o + I_r \cos(\phi - 120^\circ) \\ I_2 &= I_o + I_r \cos(\phi + 0^\circ) \\ I_3 &= I_o + I_r \cos(\phi + 120^\circ) \end{aligned} \quad (2)$$

The inferred phase is given by

$$\phi = \tan^{-1}\left(\sqrt{3}\frac{K+1}{K-1}\right); \text{ where } K = \frac{(I_3 - I_2)}{(I_2 - I_1)} \quad (3)$$

A quantitative measure of the precision with which the relative phase for a 10 mW laser can be measured is $\delta\phi \sim 10^{-7}/\sqrt{\text{Hz}}$ for a $S/N=1$.

Phase Detectors. Two detectors were used to detect the spatial heterodyne pattern phase from the interferometer. A Pulnix Model TM-7CN CCD video camera was used to display a spatial image of the fringe pattern on a TV monitor. This detector had limited dynamic range and was used for diagnostic viewing allowing the experimenter an effective method for evaluating the alignment and fringe spacing as well as the overall quality of the modulation.

The high speed detector used was a Si linear photodiode array manufactured by United Detector Technologies. The detector consisted of 76 elements 5.68 mm high and 0.310 mm pitch. Every third detector element was tied together and constituted the three signals R, S, and T. The three signals were amplified before being input to the phase processor.

The CCD camera and Si photodiode array were mounted on a common mechanical platform as seen in Figure 7. The base of the platform could be precisely translated to move one or the other of the detectors into the focal plane of the interferometer. This technique was very successful for tuning the system. The CCD camera was first slid into position; a piece of #14 welding glass was placed in front of the camera to reduce the beam intensity and ambient background light. The optics were adjusted to insure that three detector elements of the photodiode array covered one fringe cycle and that the fringe pattern was aligned with the detector elements. After the optics were satisfactorily aligned the Si photodiode array was moved into the beam and data taking was ready to commence.

Phase Processor Board. The three signals, R, S, and T from the Si photodiode array were buffered by transresistance amplifiers and fed to a novel Phase Processor Board shown in Figure 11. The phase

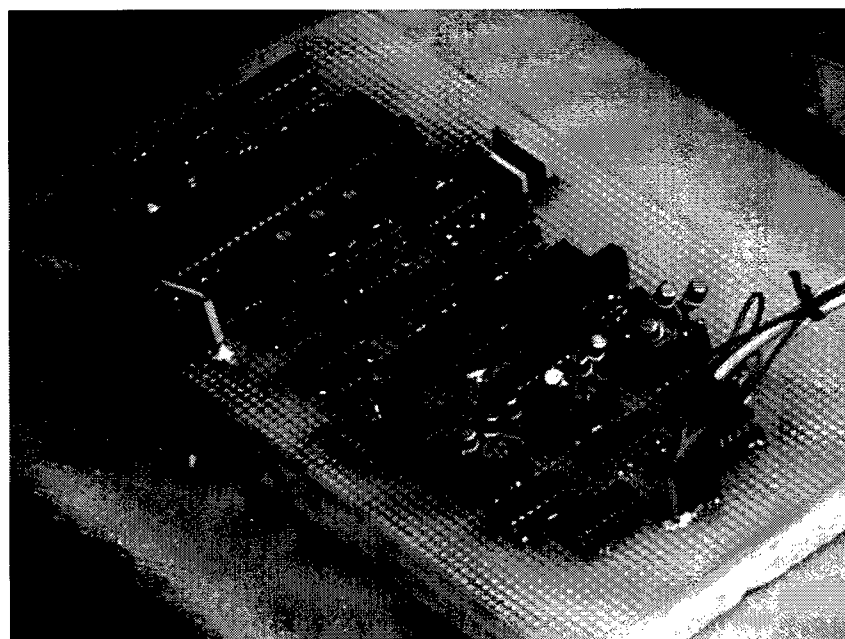


Figure 11: Photograph of phase processor board used in this experiment

processor performs three basic functions: (1) The three voltages are converted to a single digital word proportional to phase. (2) The phase is "unwrapped"; that is, cycles are counted so that the phase word is continuous over many cycles of phase change. (3) The phase data is digitally low-pass filtered to improve the signal to noise ratio of the phase data. The Phase Processor is interfaced to a personal computer via the computer's parallel (printer) port so that the phase data can be recorded and processed by the computer.

Figure 12 shows the block diagram of the phase processor. The three input voltages, R, S, and T are fed to three comparators and to a matrix of analog switches. The comparators and decoding logic determine which of the three voltages is the highest, the median, and the lowest. The switch matrix then routes those voltages to the +reference, signal input, and - reference pins of an analog to digital converter (ADC).

The digital number produced by the ADC is then given by

$$\text{digital number} = 2^n \cdot \frac{\text{middle-low}}{\text{high-low}}$$

where the resolution of the ADC, n , equals 11 for our ADC. The result is shown in Figures 13 and 14. Figure 13 shows R, S, and T as they vary over 1 cycle of phase. Figure 14 is the corresponding output

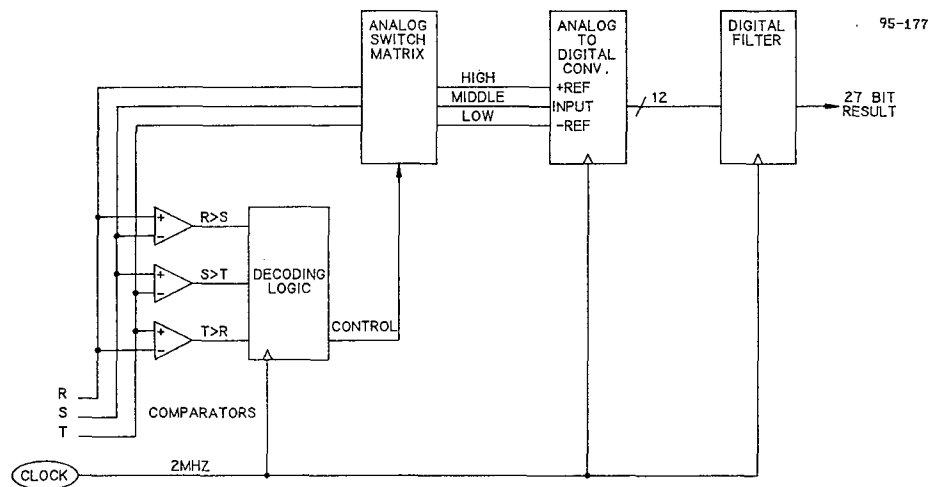


Figure 12: Functional Block Diagram of Phase Processor Board

of the ADC. The decoding logic that controls the analog switch matrix also outputs a signal that identifies the slope, positive or negative, of the waveform in Figure 13, so the phase can be uniquely determined over 1/3 of a cycle. The resolution over 1/3 of a cycle is $n+1$, or 12 bits, since each 1/6 of a cycle is digitized to the full range of the ADC.

The triangular waveform in Figure 14 is monotonically related to phase over 1/6 of a cycle, but it is not quite linear. The Phase Processor corrects for this by altering the transfer function of the ADC so that

the resultant phase word is linearized.

The 12 bit phase word is updated at the boards clock frequency of 2 MHZ. This data stream is fed into a digital filter which, in addition to filtering, performs the unwrapping function by incrementing (or decrementing, as appropriate) a counter each time the ADC output wraps around from full scale to zero or vice versa. It is important that the unwrapping function be done so that the cycle count is not lost,

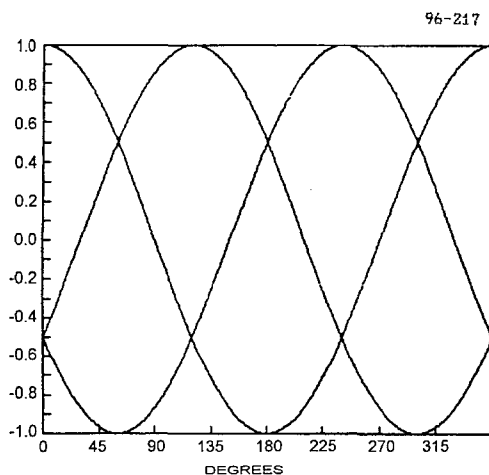


Figure 13: R, S, and T signals vs. phase

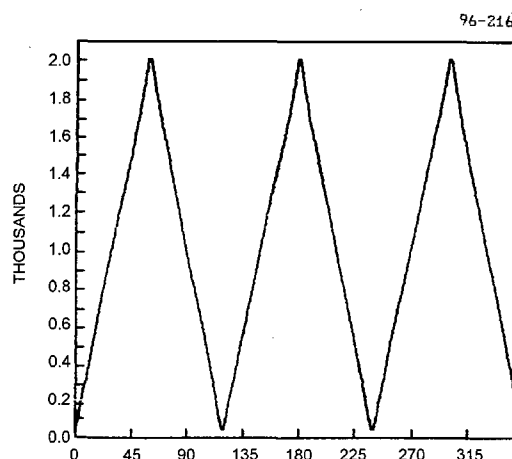


Figure 14: ADC output vs. phase (degrees)

especially if successive measurements are to be averaged. Examine what happens if the phase is near 360° and system noise causes half of the measurements to read 1° and the other half 359° . The average should be zero, but because the measurements are not unwrapped, the average is 180° , a huge error! The unwrapping process adds 360° when the phase crosses zero. The average of 359° and 361° yields the correct answer.

The digital filter has a low-pass response whose cutoff frequency f_o is given by $f_o = f_{clk}/K \cdot 2\pi$, where f_{clk} is the sampling frequency and K is a filter constant. K has a range between 0 and 2048 for this board. The digital filter allows us to extend the resolution of the phase measurement far beyond the 12 bits available from the ADC. System noise due to photon shot noise, amplifier noise, etc. acts as a dither signal to spread the signal over several ADC bins. Given that the random noise in the system is large enough to toggle the least significant bits of the ADC on successive measurements, the average over many samples can be computed to much less than 1 LSB. This allows the phase board to produce very high resolution measurements down to 1 part in 10^9 by trading bandwidth for resolution.

Laboratory Experiments:

The full design was complete and implemented four months into the effort. The mechanical design underwent two retrofits in this time: a metal skirt was added to reduce vibration, and a lens mount was added to image the fringe pattern onto the triphase detector.

Noise Characterization. The system noise from the quasi-cyclic “workstation” configuration was measured using the tri-phase detection method as part of the Phase I effort. Figure 15 is a plot of 2000 data points collected over approximately a six minute period obtained in the chemistry laboratory of Dr. Mark Nelson at the New England Medical Center. These data were obtained to represent the noise in a realistic laboratory environment where air currents and vibration from fans and people are present in contrast to the benign environment found on a floating optical bench. The phase resolution was at a typical level of $\sim 10^{-3}$ cycles. In a controlled setting an additional order of magnitude is gained ($\delta\phi \sim 10^{-4}$ cycles). Each point represents the average of 140 μ s of phase data sampled by the phase processor board at 1.37 MHz.

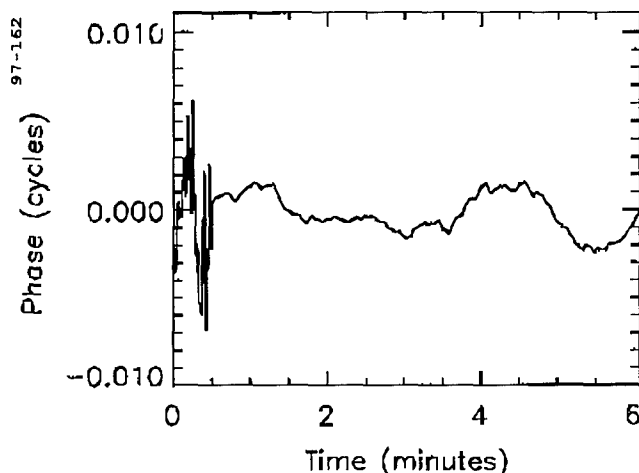


Figure 15: Typical Phase Noise Data from a realistic laboratory environment

While this is still three orders of magnitude away from the advertised phase resolution of less than 10^{-6} cycle it is already significant as an initial effort as it is a factor of 100 better than the phase resolution achieved by Schneider et al. [Schneider, 1996] using the Hartman interferometer ($\delta\phi \sim 0.025$ cycles) and 10 times better than the French group [Helmers, 1996]. Phase values at the level of $<10^{-6}$ cycles are most easily obtained using a differential measurement technique in the temporal domain as is proposed for the Phase II effort.

Protein Binding. Given the potentially low noise signature of our instrument we began measurements to observe binding events at the optical surface. Because horseradish peroxidase had served as an excellent biochemical test system, we attempted the detection of peroxidase in solution with antibody-coated waveguides. This work was delayed for some time owing to electrical failure in the laser diode, and time required for the manufacturer to replace the faulty diode.

Our signals were surprisingly weak and could not in our estimation be reliably distinguished above noise levels. The signal weakness may be understood as the consequence of a few phenomena, discussed here.

Firstly, we found after producing silane/antibody coated waveguides, that the 1.45 index of refraction BK7 glass was far from ideal given the chemistry we were using, and might only generate path length

differences on the order 1/100 cycle upon analyte binding. It is absolutely essential for the generation of larger signals, that we begin use of a higher index waveguide; 1.95 being our current figure and the index typical of the Hartman interferometer.

Secondly, we encountered difficulties with polarization artefacts. Because light of different polarizations will not interfere, our modulation efficiency was compromised.

Because of these losses, we were unable to get a large signal from the three evanescent wave/light ray interactions which occurred along each waveguide. The signal increases linearly with the number of such interactions (at scales where it is useful to model the light path as a ray) and gets very large indeed - on the order of several cycles change - when the "modal" picture is invoked and the entire optical surface resonates. Therefore, while our decision to use macroscale waveguides allowed us to demonstrate the validity of the surface chemistry and gain experience with the noise immunity of the quasi-cyclic interferometer it did provide any measurable signal.

Discussion

Noise sources. Phase measurements can be affected several different ways. The measured relative phase between the two arms of an interferometer is given by $\phi = nl\sigma$ where nl , the optical path difference between the two arms, equals the index of refraction of the target gas times the absorption path length, and σ is the wavenumber of the light ($1/\lambda$). The effects from changes in the three variables are easily seen by calculating the total derivative for $\delta\phi$:

$$\delta\phi = nl \delta\sigma + n\sigma \delta l + \sigma l \delta n.$$

In the case of a self-compensating interferometer, because the two arms are *equal by design*, the first two terms in the above equation equal zero and the phase measurement is sensitive to *only* changes in the index of refraction and insensitive to vibration, thermal variation, or changes in laser wavelength.

The interferometer constructed with Phase I resources to demonstrate the phase stability is best described as a quasi-cyclic interferometer because as was described previously, the two interferometric arms are nearly spatially identical (in order to create two independent measurement paths). While the "workstation" configuration was indeed self-compensating (demonstrated by its insensitivity to intentional changes in laser wavelength) its open optical paths were affected by turbulence and thermal gradients. A significant improvement (factor of 10) was made by constructing a plexiglass cover placed over the interferometer which reduced turbulence from local air currents, however, they were not completely erased.

Phase noise at the level of 10^{-4} cycles is not unexpected for this Phase I work. These thermal and turbulence effects typically occur on a time scale of milliseconds. In addition, overall thermal drifts coupled with the small physical separation of the two beams results in long term drifts in the phase value. These problems and others are circumvented by employing temporal discrimination on time scales faster than milliseconds. This is done by exploiting the difference in phase shifts from evanescent waves for different polarization states. Subtracting measurements of the two polarizations obtained at kHz sample

rates results in the “common mode rejection” of all slower noise sources while still providing a signal of biological origin and providing extraordinary long term stability. Visidyne has successfully used such a technique for other interferometric measurements to obtain routinely the advertised phase resolutions of 10^{-6} cycles. It is this technique that we are proposing for Phase II.

Sources of Signal Loss: The signal from the protein binding has been attenuated, as was discussed above, by three factors: Waveguide refractive index, polarization effects, and number of surface interactions.

The first of these problems is trivially addressed; glass materials which are well-characterized chemically and physically are available over a vast range of refractive indices; our preliminary information suggests that for better chemical sensing we wish to use waveguides of $n \approx 1.9$.

The second problem could be removed simply by using polarizing films at the waveguide entry and exit to select a single optical polarization throughout the experiment; while this solution is attractive, a much more elegant solution suggests itself -- we can *use* the tendency of the waveguide to alter its input polarization, to generate a differential signal. This possibility is significant and profound and is discussed further below under *Differential Measurement*.

The third problem requires fundamental alteration in mechanical design; the sensing surface must be made physically thin, less than a micron in thickness. Thick waveguides lack sufficient “optical gain” to amplify sufficiently the phase shifts, therefore, a waveguide where the total internally reflected (TIR) light “senses” the entire surface is optimum. This enhancement in conjunction with the incorporation of temporal discrimination will result in a biosensor having all of the advertised phase resolution and sensitivity.

The sensing optic must serve two purposes: it must provide a surface to physically support the receptor chemistry and it must ensure that the incident light senses the evanescent wave. This is best conceived of as a total internally reflected ray of light phase shifted with each of the thousands of encounters with the evanescent wave (i.e. bounces) incurred inside of the optic.

A planar dielectric waveguide will be constructed for the Phase II effort to take full advantage of the optical gain from thin film waveguides ($t \sim \lambda$). Figure 16 shows a slab of dielectric material (i.e. the thin film) surrounded by a cover layer (the surface chemistry and probe) and the substrate. For TIR to occur n_{film} must be greater than n_{cov} and n_{sub} .

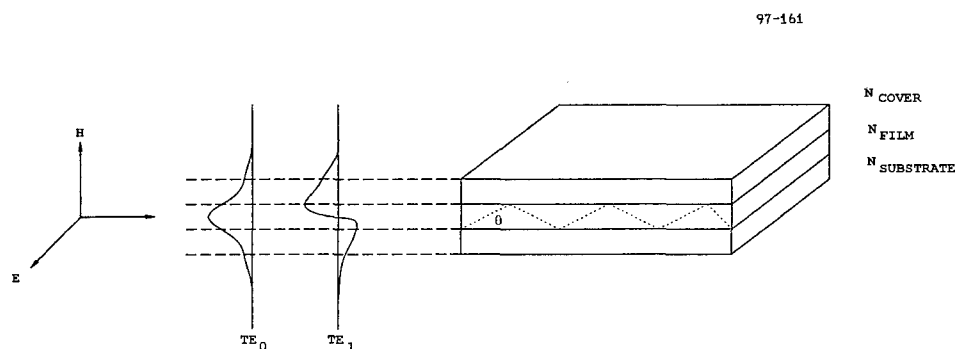


Figure 16: Schematic drawing of a planar dielectric waveguide and sample TE modes

Because the thickness of the waveguide is order of the λ , a behavior of the light within the film must be described in terms of the interacting electromagnetic fields and consequently, Maxwell's equations must be solved. When this is done it is found that a certain number of discrete modes confining the light within the n_{film} are possible. Confinement does not mean that the field is zero *at the boundary* but only that it must eventually go to zero. Therefore, the field exponentially decays to zero outside of the waveguide. This is the origin of the evanescent wave, presented from a "wave" picture rather than the simple "ray" picture invoked above.

Different modes are excited depending whether the electric or magnetic field is parallel to the boundary surface. The modes are known as transverse electric (TE) and transverse magnetic (TM), respectively, and can correspond to the orientation of the polarization of the incident light. A few of the TE field distributions are shown in Figure 16. The lowest order mode tends to travel confined primarily to the center of the waveguide while the higher order modes are concentrated more near the boundary and thus contain the most information about the evanescent wave field.

In order to increase our signal size, a thin film planar waveguide will be constructed and incorporated into the interferometer. After a suitable choice of materials and thicknesses are made, the various TE and TM modes confined within the waveguide will be calculated. The spacing (as a function of injection angle) of the different modes will be examined and specific modes or groups of modes will be selected for use. The range of angles will then be used as a guide for designing the coupling optics.

Numerous optical coating houses can produce such a device. CVI Optics, a large optical manufacturer in Albuquerque, NM have already been contacted to make the optic. The substrate material is typically made from fused silica or BK7; the surface chemistry developed during Phase I is estimated to have a similar value for its index. Therefore, the choice of material for the dielectric film is of crucial importance for TIR to occur. Typical thicknesses of 150 nm having variations of 2-3 % are routinely made; coatings with indices on the order of 1.9 are also readily available.

Several techniques are used to couple light into these thin waveguides. The optical field is the linear superposition of plane waves which in turn couple into the waveguide and excite a distribution of modes. The specific modes excited can be controlled by, for example, by matching the injection angle and polarization of the incident light to that of a specific waveguide mode. Two possible techniques for coupling the light are input coupling and prism coupling both shown in Figure 16. An example of input coupling familiar to most is light from a laser beam coupled into a single mode fiber optic cable. Input coupling launches the light directly into the waveguide by focusing the light onto the end of the waveguide. By modifying the focal length the injection angle can be adjusted.

A second method involves coupling the light into the waveguide by means of frustrated total internal reflection (FTIR) using a prism. FTIR uses the evanescent wave field as the medium for coupling the light between the prism and the waveguide. As shown in Figure 17 light is total internally reflected in a prism mounted on the waveguide surface with a small intentional gap between the two. The evanescent fields from both the prism and the waveguide couple and the light is transmitted.

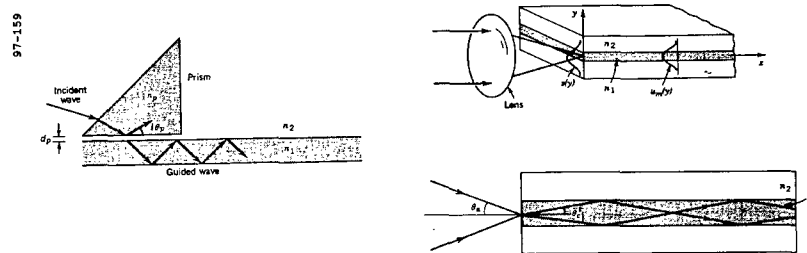


Figure 17: Methods for coupling into waveguides: at left, through a prism; at right; by focusing

Both coupling techniques will be demonstrated in the laboratory and evaluated for both stability and practical implementation in a fieldable instrument.

Quasi-cyclic physical designs we could use with miniaturized optics have been developed and some are given in our phase II proposal.

Existing Applications of Biosensors; Sensitivity Projections. Crucial to appreciating the worth of the Visidyne proposal, is an understanding of the elegance of applying Visidyne's electronics and cyclic design, to existing biosensing technology. The ensuing discussion addresses some aspects of current technology and some measurements made by that technology in order that the improvement promised by the techniques proven during our phase I work, may be assessed.

Detection and characterization of physical processes through biochemical intermediates is now routine; the strength and specificity of naturally designed reagents provide an excellent foundation for many detection processes. The idea of incorporating biomimetic sensing into an electronic device, conferring speed and ease of use, is attractive; such sensing was first performed by the creation of a glucose meter [Clark, 1962] based on currents generated by glucose oxidase. Subsequent research has focused largely on biomedical issues in part because of the easy availability of useful chemistries and expertise and in part because the market is expected to be excellent.

Diverse chemistries and electronics have been applied to the construction of biosensors [McCormack, 1995]. The general constructions have been either amperometric or potentiometric sensors based on redox chemistry, FET sensors based on surface charge accumulation by receptor-ligand coupling, piezoelectric sensors based on mass accumulation by receptor-ligand coupling, and optical sensors. Each approach has met with varying degrees of success.

Optical methods in particular have revolutionized chemical sensing much as they have revolutionized telecommunications. Optical fibers can monitor changes in absorbance, reflectance, and fluorescence and their small diameter and flexibility confer great potential for continuous sensing in poorly accessible or remote sites. Furthermore, optical fibers neither create nor detect electromagnetic interference, can be simple in design, are conducive to miniaturization, and are low in cost, making feasible disposable sensors for sterile applications. The technology for tethering reagents onto glass has now become quite sophisticated and the possible surface chemistries of an optic are vast and continually growing through the inventive work of sensor chemists. Lateral evanescent wave coupling has been partially explored; this work in general relies not on the phase shift of the transmitted wave, as would our system, but rather on the introduction of fluorescent agents onto the analyte. This method is attractive because it has potential for multianalyte sensing but gives poor signal-to-noise relative to our proposed technique and imposes further limits on the detectable analytes.

The most sensitive optical biosensors currently on the market are surface plasmon resonance (SPR) detectors. Two are commercially available: the BIAcore system developed by Sweden's Pharmacia and now marketed by BIAcore, Inc., and the IAsys resonant mirror biosensor from Britain's Affinity Sensors. Both techniques rely on the change in absorbance of a resonating surface -- gold film for the BIAcore and a monomode waveguide for the IAsys -- to which detecting macromolecules or ligands have been tethered. These devices have been used for a variety of applications, including detection of protein-nucleic acid interactions, receptor-ligand interactions, antibody-antigen binding, and real-time observance of nucleic acid hybridization kinetics; these measurements are based on power of the absorbed signal and not on phase. These instruments are physically large and prices run upwards of \$250,000; significantly, they are generally usable only down to about $10^{-1}K_d$ -- that is, *four orders of magnitude* less sensitive than the phase-based sensor we propose here. The "dipstick" nature of the proposed Visidyne device brings to the field portability, ease of use, suitability for stopped flow kinetic measurement, low price, and shot noise limited sensitivity. Consequently, our proposed sensor appears to have little serious competition and a large, pre-existing market.

The BIAcore in particular, despite its poor sensitivity when compared against our proposed sensor, has found widespread use as a research tool and is used in over 500 papers in the peer-reviewed scientific literature. It requires a large carefully designed housing and setup, and is therefore entirely unsuitable

for field use. It is a power, not a phase, measurement, and so cannot use “optical subtraction” as we propose to evade nonspecific artefacts. Even so, it has already been used in a vast number of experiments published in the literature. BIAcore analysis has been used to characterize protein/protein and protein/DNA interaction for transcriptional activators, receptor-ligand interactions, signal transduction intermediates, and all over biochemistry. It has *not* been used for detection of pathogenic organisms (bacteria or viruses) because the UV wavelengths the SPR phenomenon requires do not allow a large enough evanescent wave penetration; the IR wavelengths we are using thus add functionality.

Of particular relevance to this SBIR effort are some uses of the BIAcore evanescent wave sensor in sequence-specific detection of nucleic acids. Examine the data in figure 18. Here we see BIAcore detection [BIAcore application note 306] in which a single-stranded, biotinylated nucleic acid, tethered to the surface of the detector through a streptavidin mediator (not unlike our chemistry), is hybridized to its complementary sequence, or to a sequence containing a single G to C mismatch. The target concentration is a whopping 800 nM and the conditions are stringent, with high temperature and salt. What is immediately apparent is the poor ability to distinguish the target sequence for mismatches. The distinction improves as the probe is shortened -- since a single mismatch among 13 bp is more crucial than a single mismatch among 27 -- but there is clearly a real difficulty with nonspecific binding. The inherent dual-beam nature of the Visidyne interferometer, as explained above, circumvents this difficulty; by placing closely related sequences on the reference arm the specific allele desired can be targeted, trading sensitivity and specificity to meet the needs of a particular application. Note also that we offer at least *four orders of magnitude* greater sensitivity -- more of the analyte makes use of the additional volume spanned by the IR evanescent wave -- which means, we would expect the same clear signal-to-noise ratio at a DNA concentration of only 80 pm or better.

The clear signal and sensitivity of the BIAcore makes possible the direct observation of molecular biological processes. The experiment [BIAcore Application Note 901] whose results are shown in figure 19 is particularly appealing and if time permits Visidyne would like to attempt something similar in the Phase II process simply for its pleasant clarity as a demonstrational tool.

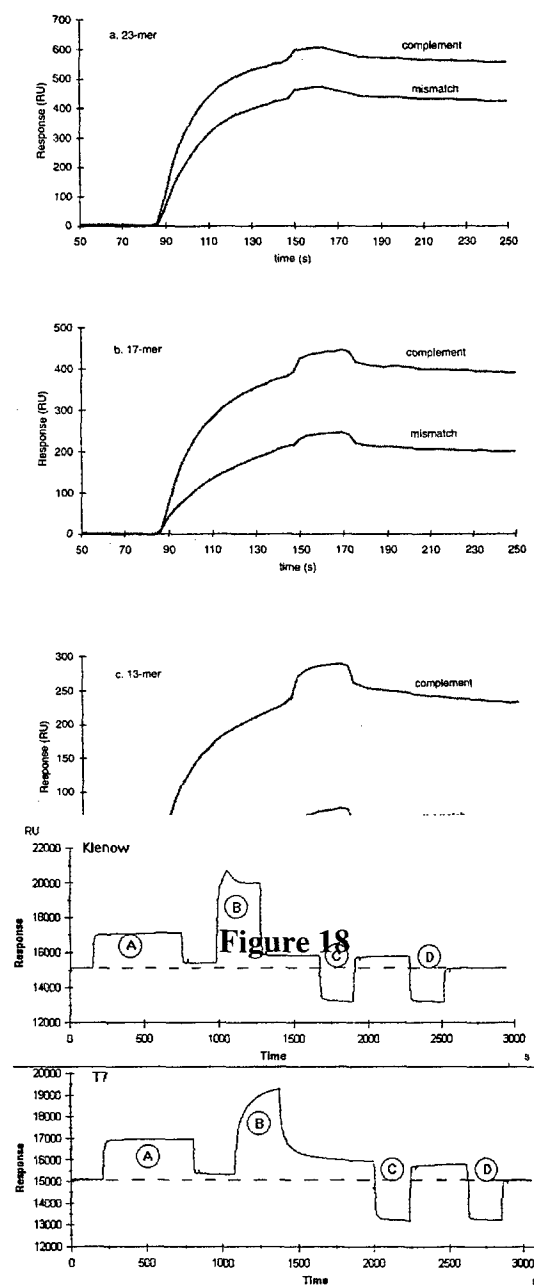


Figure 19

Here, the instrument again begins with a single-stranded nucleic acid (in this case a 69-mer) attached to the optical surface, again through a biotin/avidin coupling. Signal (A) is generated by the hybridization of a 23-mer to the 3' end of the tethered oligo, generating a primer with a free 3' phosphate for DNA synthesis -- a nice clear signal is observed as the second strand hybridizes; this the kind of signal we expect from viral RNA detection. At (B), polymerase is added to the sensor along with a mix of all four deoxynucleotides -- Klenow in the top figure, T7 in the bottom figure; the signal enables *actual visualization of DNA synthesis taking place on the sensor surface* -- it is interesting to note that the different kinetics of the T7 and Klenow polymerases are here visible; even the "overshoot" in the Klenow fragment's signal is reproducible. If T7 is added without deoxynucleotides the investigators report a small signal due to polymerase binding at the sticky end, with no subsequent elongation. At (C), SDS is added to wash off residual polymerase, and is then flowed out; the resultant offset from baseline represents the difference in signal from before hybridization, to after hybridization with all attached protein gone. At (D), alkali is pulsed through the sensor to melt the strands -- note that after the pulse the signal returns to baseline, corresponding to a return to the original chemical configuration.

The BIAcore is only one evanescent wave sensor, though perhaps as yet the most commercially successful one. A group at Georgia Tech, and their corporate partner, Photonic Sensor Systems, has been experimenting successfully with a device very similar to the one described here; an evanescent wave biosensor measuring phase shifts in near infrared light from diode laser sources. Their system has some disadvantages and advantages over ours: as an advantage, they have already developed a miniaturized system, as Visidyne proposes to do as part of the phase II work: thus they are operating in the "modal" configuration described above, with *thousands* of reflections occurring rather than two or three, and hence get much larger signals. The group has also begun working with higher-index waveguides, which provide an additional large amplification to their signal; Visidyne has only proposed to obtain high-index glass as part of the Phase II work, since the Phase I work has indicated that this glass will be essential. However Photonic Sensor Systems has no special technology for measuring phase, comparable to the three-signal phase processor Visidyne brings. Rather, the Georgia Tech group's approach is simply to observe the generated phase with a CCD camera. This crude technique gives resolution less than 1/100 of a fringe -- and that only when the physical environment of the sensing chip becomes constrained into tightly recessed channels which do not properly mix with solution. Already *two orders of magnitude* less sensitive than the Phase I detector, and *five orders of magnitude* less than a differential technique would allow. In addition the Photonic Sensor Systems group reports severe problems with DC signal offsets -- to which the Visidyne technique is immune -- and with thermal and vibrational noise, to which the phase I work proves the Visidyne "quasi-cyclic" design is immune. In addition Photonic Sensor Systems has not yet fully exploited the opportunity to correct for nonspecific events, and the noncyclic nature of their interferometer makes such correction impossible anyway: the paths must be equivalent for one to correct the other.

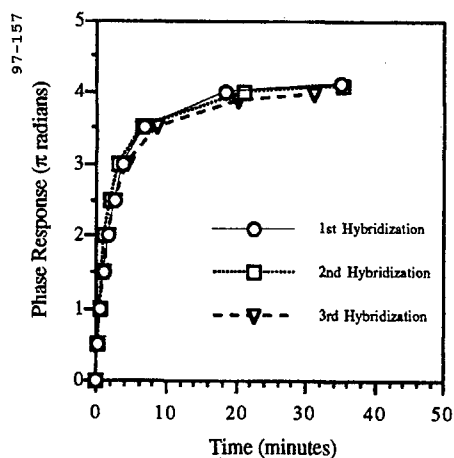


Figure 20

Nonetheless, the physical basis of the Georgia Tech signal is identical to ours. They have also developed a single-stranded, sequence specific nucleic acid detector; as ours, it couples a probe onto the glass surface through a protein mediator (avidin, not an

immunoglobulin -- see "Chemical design" above for a discussion) and so are at less than their optimal sensitivity. Figure 20 shows data from Photonic Sensor Systems, in which the target 37 base oligonucleotide was hybridized onto the 37 base ss probe on the sensor. The target was then melted off with 50 mM NaOH and rehybridized twice -- each time the signal was as strong as the first time, indicating the reusability of this chemistry. The detection threshold for this sensor was as low as 0.5 ng/mL and was limited by the optics [personal communication from Dr. Nils Hartman of Georgia Tech research Institute]. That means that Visidyne's optical sensitivity could correspond to chemical sensitivity of 0.5 pg/L or even 5 pg/kL -- PCR-like sensitivity!

A French group [Helmets, 1996] has also designed a refractive-index based chemical sensor; their sensor, which makes no correction for nonspecific artefacts, is enveloped in a polymer which swells in the presence of gaseous hydrocarbons and is not a biosensor *per se*; it does however represent an area of use for our sensor. Their data are shown in fig. 21. Note that their signal is approximately linear in gas concentration and is on the order of two whole cycles (~12 rad); their detection on these data apparently fades away at about 1/10 of a cycle (0.6 rad). Thus Visidyne's phase resolution of 10^{-7} cycle in real time, could be an extremely effective warning system for environmental hazards or toxic gases, measuring toxic fumes down in the *parts-per-billion* region.

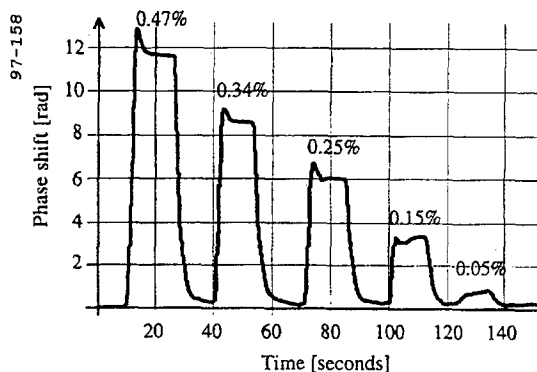


Figure 21

Thus, with little or no change in existing mechanical and chemical devices, Visidyne's *existing, proven* electronics hold out the promise of a needed device, broad and immediate in application.

Differential measurement: Visidyne has formulated a strategy to enhance the signal, and reduce the noise, seen during the phase I trials; this strategy can be found separately in our phase II proposal to DoD. However we would like to present here an aspect of this strategy, a bandpass filtering technique unique in the field of biosensing and offering extreme advantages over any optical biosensing scheme of which we are aware; the development of this technique represents a contribution to optical biosensing as significant as Visidyne's phase measurement technique and is a major result of the phase I feasibility study.

Temporal Discrimination. The majority of the phase noise is caused primarily by thermal gradients and vibrations which typically occur on millisecond timescales and longer. For example, a common problem with interferometric biosensor is an increase in the base value of the phase (the "dc" value) caused by slow ambient thermal drifting or vibrations from laboratory fans. While careful optical design can remove a significant portion of this noise, at the proposed phase resolution levels ($<10^{-6}$ cycles), this is most effectively done by finding a temporal discriminant and using it to bandpass filter any noise sources occurring on timescales slower than the sampling rate.

The polarization of the incident light can be used as just such a discriminant. As was previously discussed, the phase shift associated with TIR has a different value depending on the source orientation. In a thin film planar waveguide this corresponds to alternately exciting TE and TM modes.

Consequently, by switching between the two linear polarizations at kHz rates and subtracting the respective measurements, any noise common to both measurements will be removed and only the relevant biochemical phase information remains.

Bandpass Filtering. This novel method of bandpass filtering out noise sources is described using data obtained from an interferometer employing changes in wavelength instead of polarization as the temporal discriminant. The power spectral density (PSD) from an unequal path Mach-Zehnder interferometer was measured and is shown in Figure 22. The noise power density falls off with higher frequency. The phase

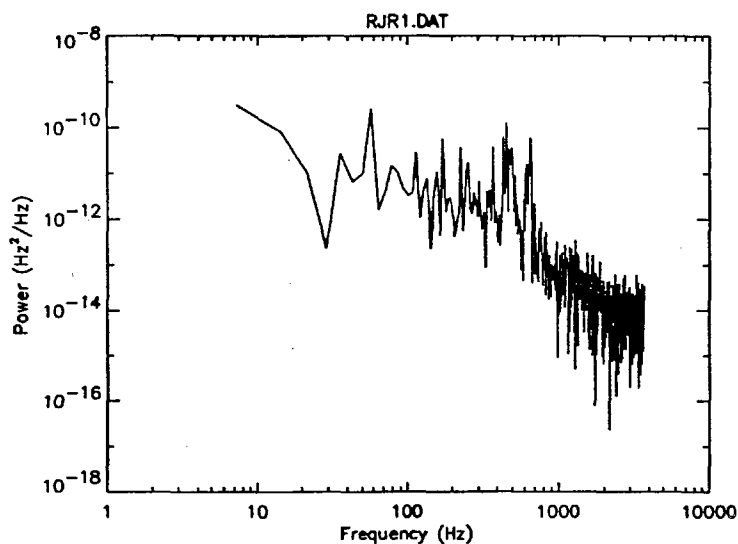


Figure 22: System Power Spectral Density

resolution amplitude (square root of the power density) equals $\sim 10^{-7}$ Hz/ $\sqrt{\text{Hz}}$ at 1 kHz, a factor of 100 less than at 10 Hz.

Since the noise floor (which corresponds to the best possible phase resolution) is reached at a ~ 1 kHz, there is no benefit to be gained by sampling faster. The shape of the noise power spectrum can be taken advantage of by tailoring a bandpass filter to select specific information as is shown below. In this laboratory work the current of the laser diode was modulated with a square waveform dithering the wavelength of the laser at a rate of 7.5 kHz. Phase data were recorded in pairs corresponding to the two current levels. The two phase values were then subtracted from each thus removing the lower frequency noise common to both signals. A plot of the PSD for this is shown in Figure 20. The low frequency values are seen to be attenuated by a factor of 10^4 in power indicating the effectiveness of this technique.

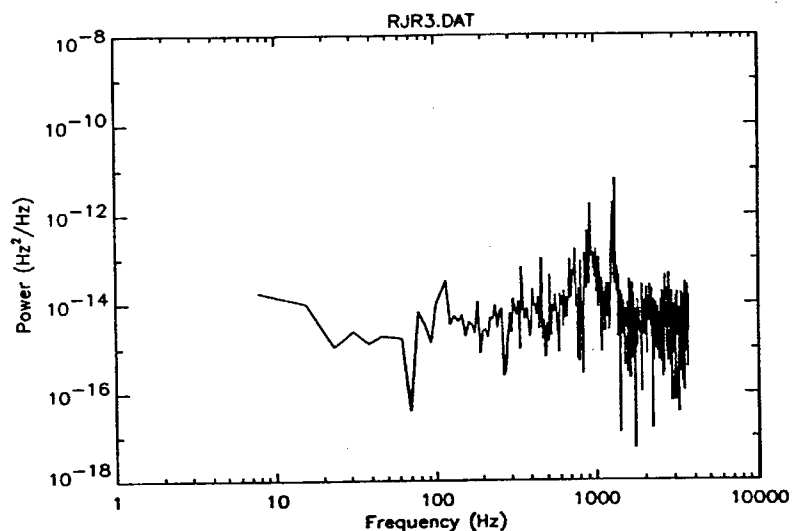


Figure 23: Bandpass filtered power spectral density

A plot of the corresponding phase measurement values is shown in Figure 24. The data are presented as a histogram of 500 of these differential measurements and can be interpreted as the statistical spread in any single measurement. *The ensemble of 500 points was taken continuously over a total time of 8 minutes under less than ideal circumstances thus demonstrating its extraordinary immunity to noise and remarkable stability for field applications.* Each point of the ensemble of *measured data* corresponds to ~0.25 seconds (the average of 1000 differential pairs) and demonstrate the advertised phase resolution. The interpretation of this plot is as follows: each phase measurement obtained with the interferometric system has an uncertainty of $\pm 1 \times 10^{-7}$ cycles/ $\sqrt{\text{Hz}}$ associated with it. A phase measure having a resolution of 10^{-7} cycles can be obtained by collecting data for one second.

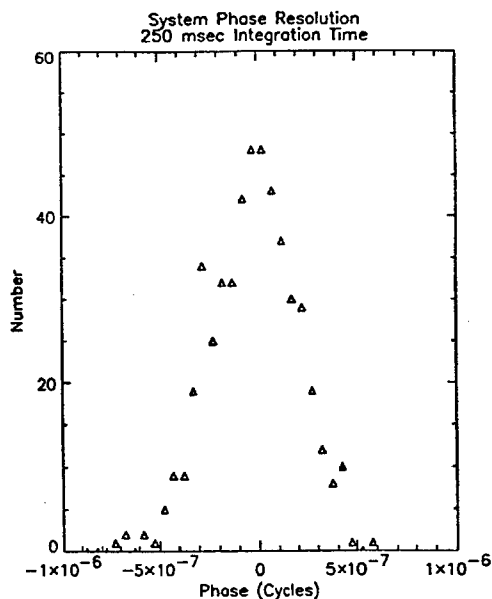


Figure 24: Phase measurement obtained with a Visidyne precision phase detector.

In Phase II this differential technique will use polarization effects in place of wavelength variations to interrogate changes to the evanescent wave. Specifically, the polarization of the laser diode will be modulated between the two orthogonal linear polarizations alternating excitation of TE and TM optical modes within the waveguide. The corresponding two phase measurements will be subtracted hence removing any common noise and isolating the target signal due to the change in δn_{bios} at a specific sampling frequency.

Polarization Modulators. Key to successfully implementing this technique is the introduction of a polarization modulator. Photoelastic modulators and ferroelectric liquid crystal switches are two excellent candidates for modulating or varying (at fixed frequency) the polarization of a beam of light. Each device operates on an electro-optic principle - introducing birefringence through compression in the photoelastic case and reorienting the ferroelectric domains through application of a field in the liquid crystal case. Both modulators have response times on the order of 20 μs (50 kHz) and are transparent at visible wavelengths making them compatible with the proposed effort. Both devices also are available as off the shelf items and require a small controller for operation.

Photoelastic modulators are available from Hinds Instruments in Hillsboro, OR; ferroelectric liquid crystals are available from several manufacturers such as Meadowlark Optics and Displaytech. Visidyne will evaluate each device for efficiency, size, cost, and ruggedness and purchase the best modulator. The modulator will then be introduced into the interferometer (following the laser diode) and the subsequent phase measurements will be synchronized to the modulation between linear polarizations.

Conclusions:

Visidyne has made great strides in implementing new optical and electronic techniques for this proposal, and we have demonstrated well that our technology can be grafted onto existing technology. Our chemistry and biochemistry have been commensurate with the best in the field and our physical sensitivity vastly outpaces the field. However there is a great deal of technical mastery required for this effort, and the extremity of our precision subjects our sensor development to novel challenges. Consequently we were unable to fulfill the phase I work plan, which was ambitious in that it wished to have finished, within six months, with Visidyne already able to make RNA detection measurements of unparalleled sensitivity and speed. Nonetheless, as a consequence of the phase I effort all the necessary components of the system have identified and proven. In addition, Visidyne has established that it can make innovative and remarkable contributions to the field, through tri-phase detection, differential measurement, and chemical self-correction. Visidyne is now confident that the remaining development consists of *assembling* these discretely proven technologies; while this challenge is not insignificant it is a straightforward and solvable problem of interfacing different pieces of a functioning system. Our confidence in this effort is therefore sufficient that we are continuing to fund this development internally and seeking further external funding sources, including the submission of a Phase II proposal for this work.

References

Abraham, R., Chonmaitree, T., McCombs, J., Prabkhar, B., Lo Verde, P., and Ogra, P., "Rapid Detection of Poliovirus by Reverse Transcription and Polymerase Chain Amplification: Application for Differentiation between

Poliovirus and Nonpoliovirus Enterovirus.," *J. Clin., Microbiol.*, **31**, 395-399, 1993

Clark, Jr., L. C., and Lyons, C., "Electrode Systems for Continuous Monitoring in Cardiovascular Surgery," *Ann. NY Acad. Sci.*, **102**:29-45, 1962.

Egger, D., Pasamontes, L., Ostermayer, M., and Bienz, K., "Reverse Transcription Multiplex PCR for Differentiation between Polio and Enteroviruses from Clinical and Environmental Samples," *J. Clin. Microb.*, **33**, 1442-1447, 1995

Helmers, H., Greco, P., Rustad R., Kherrat R., Bouvier G., Benech G., "Performance of a Compact, Hybrid Optical Evanescent-Wave Sensor for Chemical and Biological Applications", *AO*, **35**, 1996.

McCormack, doctoral dissertation: "Development of an optical Immunosensor Based on the Evanescent Wave Technique," School of Biological Sciences, Dublin University, 1995.

Meselson, M., Guillemin, J., Hugh-Jones, M., Langmuir, A., Popova, I., Shelokov, T., and Yampolskaya, O., "The Sverdlovsk Anthrax Outbreak of 1979," *Science* **266**: 1202-1208, 1994.

Rieder, R.J., "High Sensitivity Water Vapor Measurements from Phase Determination, NASA Phase I SBIR Final Report", *Visidyne Report No. VI-2544*, (1995).

Schneider, B.H., Shafer, D. A., and Hartman, N. F., "Integrated Optic Interferometer for the Direct Detection of Nucleic Acids," Poster presented ACS meeting, San Francisco, CA, April 13-17, 1997.

Wang, J., Palecek, E., Nielsen, P., Rivas, G., Cai, X., Shirashi, H., Dontha, N., Luo, D., and Farias, P., "Peptide Nucleic Acid Probes for Sequence Specific DNA Biosensors," *J. Am. Chem. Soc.*, **118**, 7667-7670 1996

Zehnpfennig, T. F., "Precision Reference Subsystem for Head-Mounted Displays", SBIR Final Report, *Visidyne Report No. VI-2714*, (1995).

Personnel:

A list of the individuals responsible for the work performed on the project follow. Dr. Ronald Rieder, PI, had primary responsibility for any optical considerations as well as for the overall technical management of the program. Mr. Sanjay Krishnaswamy primarily responsibility was for all biochemical considerations as well as carrying out a significant amount of all laboratory work. Mr. Jeff Gourde was responsible for any mechanical engineering and the fabrication of the interferometer. Dr. Mark Nelson, consultant, was responsible for the chemistry protocol and its subsequent development. Dr. Alfred Ducharme and Mr. Peter Baum assisted with electrical engineering aspects of the project.



DEPARTMENT OF THE ARMY
US ARMY MEDICAL RESEARCH AND MATERIEL COMMAND
504 SCOTT STREET
FORT DETRICK, MARYLAND 21702-5012

REPLY TO
ATTENTION OF:

MCMR-RMI-S (70-1y)

4 Dec 02

MEMORANDUM FOR Administrator, Defense Technical Information
Center (DTIC-OCA), 8725 John J. Kingman Road, Fort Belvoir,
VA 22060-6218

SUBJECT: Request Change in Distribution Statement

1. The U.S. Army Medical Research and Materiel Command has reexamined the need for the limitation assigned to technical reports written for this Command. Request the limited distribution statement for the enclosed accession numbers be changed to "Approved for public release; distribution unlimited." These reports should be released to the National Technical Information Service.

2. Point of contact for this request is Ms. Kristin Morrow at DSN 343-7327 or by e-mail at Kristin.Morrow@det.amedd.army.mil.

FOR THE COMMANDER:

Encl


PHYLLIS M. RINEHART
Deputy Chief of Staff for
Information Management

ADB218773	ADB229914
ADB223531	ADB229497
ADB230017	ADB230947
ADB223528	ADB282209
ADB231930	ADB270846
ADB226038	ADB282266
ADB224296	ADB262442
ADB228898	ADB256670
ADB216077	
ADB218568	
ADB216713	
ADB216627	
ADB215717	
ADB218709	
ADB216942	
ADB216071	
ADB215736	
ADB216715	
ADB215485	
ADB215487	
ADB220304	
ADB215719	
ADB216072	
ADB222892	
ADB215914	
ADB222994	
ADB216066	
ADB217309	
ADB216726	
ADB216947	
ADB227451	
ADB229334	
ADB228982	
ADB227216	
ADB224877	
ADB224876	
ADB227768	
ADB228161	
ADB229442	
ADB230946	
ADB230047	
ADB225895	
ADB229467	
ADB224342	
ADB230950	
ADB227185	
ADB231856	